

MAORY optical design analysis and tolerances

M. Patti*^a, M. Lombini^a, D. Magrin^b, D. Greggio^b, E. Diolaiti^a, F. Cortecchia^a, C. Arcidiacono^a, P. Ciliegi^a, P. Feautrier^c, R. Ragazzoni^b, S. Esposito^d

^aINAF – Osservatorio di Astrofisica e Scienza dello spazio, via Gobetti 93/3, 40129 Bologna (Italy); ^bINAF – Osservatorio Astronomico di Padova, Vicolo Osservatorio 5, 35122 Padova (Italy); ^cInstitut de Planétologie et d’Astrophysique de Grenoble, 414, Rue de la Piscine, Domaine Universitaire, 38400 St-Martin d’Hères (France); ^dINAF – Osservatorio Astrofisico di Arcetri, L.go E. Fermi 5, 50125 Firenze (Italy)

* mauro.patti@inaf.it; phone +39 051 63573 315

ABSTRACT

MAORY (Multi-conjugate Adaptive Optics RelaY) will be the multi-conjugate adaptive optics module for the ELT first light. MAORY is a post focal relay optics and supports the MICADO imager and spectrograph.

The tolerance process of MAORY is one of the most important step in the instrument design since it is intended to ensure that MAORY requested performances are satisfied when the final assembled instrument is operative. At the end, the assignment of tolerances to the various opto-mechanical parameters should be a trade-off between final cost of the system and its resulting performances.

This paper describes the logic behind the tolerance analysis starting from definition of quantitative figures of merit for MAORY requirements and ending with estimation of MAORY performances perturbed by opto-mechanical tolerances. The method used to estimate tolerances takes care of compensation of errors during assembly/alignment procedure and uses a Root-Sum-Squared (RSS) merit function to combine independent error contributions. There are two requirements that limit the allowable changes of opto-mechanical parameters. The Root-Mean-Squared wavefront error (RMS WFE) and the optical distortion. The first one must satisfy diffraction limited performance over the MICADO Field-of-View (FoV) while the second one must satisfy high astrometric accuracy and precision. As criterion for tolerancing, the defined merit function considers the RMS wavefront referred to star centroids and adds boundary constraints on the compensators and geometric distortion in MICADO FoV. To evaluate the impact of tolerances on astrometry, a Monte Carlo approach was followed validating the expected performances from a pure opto-mechanical point of view.

--

Keywords: Tolerance, Extremely Large Telescope, Optics, Astrometry

1. INTRODUCTION

MAORY [1] will be the multi-conjugate adaptive optics module for the Extremely Large Telescope (ELT) [2] first light. MAORY is a Post-Focal Relay Optics and shall deliver high performance astronomical observations to the MICADO [3] (MCAO Imaging Camera for Deep Observations) imager and spectrograph. To support the MICADO near-infrared camera, MAORY provides two adaptive optics modes. The first is a multi-conjugate adaptive optics (MCAO) mode; the second is a single conjugate adaptive optics (SCAO) mode.

At first light, MAORY will contain a single deformable mirror with provision for a second deformable mirror as an upgrade. In the MCAO mode, at least one deformable mirror (DM) within MAORY works together with M4, a DM inside the telescope and conjugated to the ground. The DMs are conjugated to different altitudes to provide a wide FoV with high Strehl ratio and uniformity of the point spread function (PSF). The SCAO mode will deliver high Strehl ratio for a smaller field, rather than uniform Strehl ratio over a wide field. To deliver the performance required by the MICADO science case, MAORY uses six laser guide star (LGS) wavefront sensors (WFS) and three natural guide star (NGS) wavefront sensors in the MCAO mode, while the SCAO mode, as defined, works on a single bright natural star.

The current baseline optical design of MAORY [4] is based on six mirrors (including one or two adaptive mirrors) and a dichroic beam-splitter. This dichroic beam-splitter is used to split the science light from the LGS light that is transmitted to the LGS WFSs by means of a focusable objective [5].

The tolerance analysis of MAORY Post-Focal Relay Optics has been necessary to establish part of the system error budget. One possible way to establish the tolerance budget is an iterative analysis of the optical system performances described as follows:

1. Select a preliminary tolerance budget.
2. Perform the sensitivity analysis.
3. Compute RSS for all the aberrations for each individual tolerance. This will indicate the relative sensitivity of each tolerance.
4. Compute RSS for all the effects calculated in step 3 combined.
5. Compare the results of step 4 with the performance required of the system.
6. Adjust the tolerance budget so that the result of step 5 is equal to the required performance. Since the larger effects dominate the RSS, tighten the most sensitive tolerances. Conversely, one should be sure that the tolerances are not tightened beyond a level at which fabrication and/or alignment precision becomes impossible.
7. After few iterations (steps 2 through 6) the tolerance budget should converge to one which is acceptable in terms of performances and reasonable in term of costs. If the tolerances necessary to get acceptable performances are too tight to be fabricated, one way to ease the problem is to add compensators and set allowable ranges for the compensators: they can be adjusted to match the required performances.

This is the basic logic behind the tolerance analysis described in the present document, where:

- Section 2 summarizes the principal requirements that lead the instrument design and constrain the tolerance analysis.
- Section 3 describes the tolerance analysis breakdown and the effect of tolerances on the expected performances of MAORY.
- Section 4 summarizes the results.

2. MAORY POST-FOCAL RELAY OPTICS

2.1 MAORY optical design overview

A detailed description of the Post-Focal Relay Optics sub-system of MAORY can be found in Lombini et al. [4]. This section gives a brief summary of the baseline design.

The Post-Focal Relay Optics re-images the telescope focal plane to the exit ports. The sub-system contains the following channels:

- **Main Path Optics**, which relay the telescope focal plane to the exit ports for the science instruments (MICADO and 2nd instrument as yet undefined);
- **LGS Objective**, which creates an image plane for the LGSs, used by the LGS WFS sub-system to measure in real-time the high-order wavefront aberrations for the MCAO mode of MAORY.

Inside the optical path, two clear planes are created, optically conjugated to two different ranges from the telescope entrance pupil, allowing the insertion of up to two deformable mirrors (DMs).

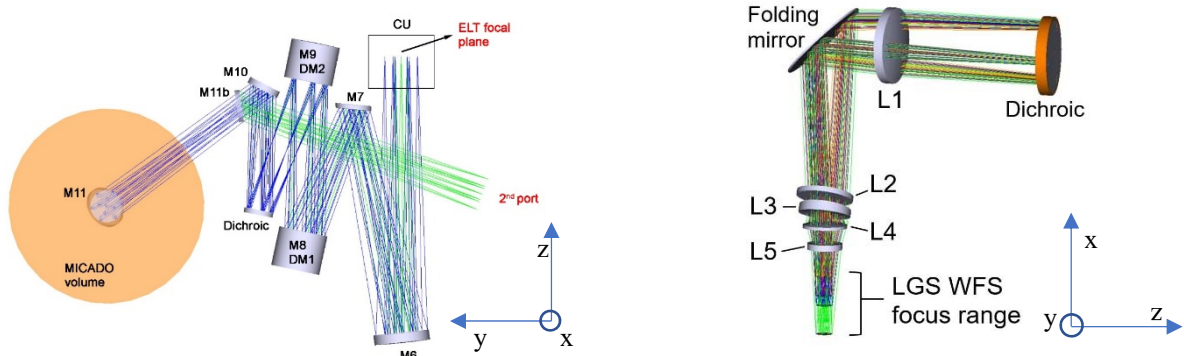


Figure 1. Left: Main Path Optics layout. Blue rays: optical beam from telescope focal plane to exit port for MICADO. Green rays: differential path to exit port for second instrument. Right: LGS Objective layout.

The Main Path Optics, shown in Figure 1, consist of 6 mirrors (M6 to M11: numbering starts with M6 to take into account the first 5 mirrors, which form part of the telescope optics) and the LGS Dichroic, which splits the light beam into two channels: the reflected light beam (“science path”) is transferred to the exit ports, the transmitted light beam (“LGS path”) is focused by the LGS Objective.

Mirror M11 is shown in two copies: M11 and M11b, corresponding to two different exit ports. Mirror M11b is deployable: it is normally out of the beam to let the light propagate to mirror M11.

Mirrors M8 and M9 are intended to be DMs for adaptive optics compensation of the optical wavefront. As such, they would be out of the scope of the present document. However, in a partial implementation of the instrument, at least the deformable mirror M9 would be replaced by a rigid mirror. Moreover, it is of interest to evaluate the feasibility and cost also of mirror M8, for instrument test purposes. For these reasons, also mirrors M8 and M9 are described here. For the scope of this document, they should be intended as rigid mirrors.

The LGS light propagated through mirrors M6, M7, M8 (DM) and M9 (DM) is transmitted by the LGS Dichroic, which is located close to a pupil plane, and is focused by the LGS Objective to create an image of the 6 LGSs for the LGS WFS sub-system.

The LGS Objective is designed to have a minimum focus distance of 80 km. The output focal ratio of F/5 allows reasonable motion of the exit image plane, as the image of the sodium layers varies.

The 6 LGSs will be launched from the edge of the primary ELT mirror and they rotate as the Zenith angle of observation. Their image plane shifts along the optical axis due to the variation of the mean distance of the LGS from the telescope which is inversely proportional to the cosine of the Zenith angle.

The LGS Objective, shown in Figure 1 consists of five lenses and a flat mirror. The baseline material for all refractive elements is optical glass (BK7, S-BSL7 or equivalent glass).

The last part of the optical axis is folded by the flat mirror, so that the LGS WFS sub-system is mounted in gravity invariant configuration.

2.2 Main Path Optics wavefront error

The RMS WFE at the exit focal plane of the Main Path Optics is shown in Figure 4. The off-axis mirrors are decentred and tilted in one axis only, hence the WFE map is symmetric along the other axis. The NGS patrol FoV and MICADO science FoV have been considered in the analysis of RMS WFE. In the tolerance analysis, the goal was to keep the RMS WFE below the diffraction limit within MICADO FoV at wavelength $\lambda = 1\mu\text{m}$.

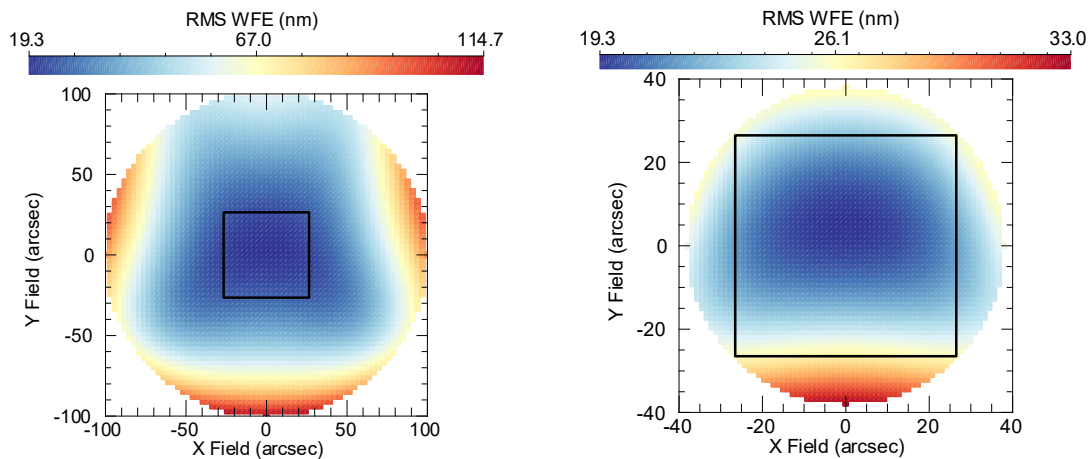


Figure 2. RMS WFE without degradation from manufacturing and alignment errors; nominal telescope design included. Left: RMS WFE maps of the entire MAORY FoV. Right: RMS WFE maps of MAORY within the MICADO FoV. The black square is the 53”x53” MICADO detector.

2.3 Main Path Optics geometric distortion

MAORY/MICADO astrometry requires observations to be taken at different epochs in order to detect motions of astronomic sources, either with the motions of the science objects relative to each other or with respect to the sky coordinate system (or both). There are two categories of astrometric observations:

1. Intra-epoch observations are those for which the science and/or reference objects can be considered stationary. If motions of science objects were detected, they would be caused by measurement errors.
2. Inter-epoch observations are those for which the science and/or reference objects cannot be considered stationary. These are the observations used to determine the motions of science objects.

MAORY shall permit inter-epoch observations such that the relative position on the sky of an unresolved, unconfused source of optimal brightness with respect to an optimal set of reference sources must be reproducible to within 50 μs (goal: 10 μs) over a central, circular field of 20 arcsec diameter (goal: 75 arcsec diameter).

The positions of a set of N test stars placed over a regular square grid has been used to evaluate the astrometric residual error. Let's define X_{inp}, Y_{inp} as initial coordinates of star centroids. X_o, Y_o are coordinates of the star centroids after a given FoV rotation angle. Considering a range of field rotations in the circle containing the MICADO FoV, the distortion has been estimated and corrected using a n^{th} order polynomial of the form:

$$X = \sum_{i,j} Kx_{i,j} X_o^i Y_o^j \quad (1)$$

$$Y = \sum_{i,j} Ky_{i,j} X_o^i Y_o^j \quad (2)$$

Where n^{th} order indicates the max of the sum of the exponents i and j in the equations. The $Kx_{i,j}$ and $Ky_{i,j}$ are $(n+1)$ square matrixes used to model the distortions introduced by the optics after a given FoV rotation angle. The X, Y coordinates have been compared to X_{inp}, Y_{inp} in order to compute polynomial fit error. The final error in the position is the standard deviation computed as the quadratic sum of $(X - X_{inp})$ and $(Y - Y_{inp})$.

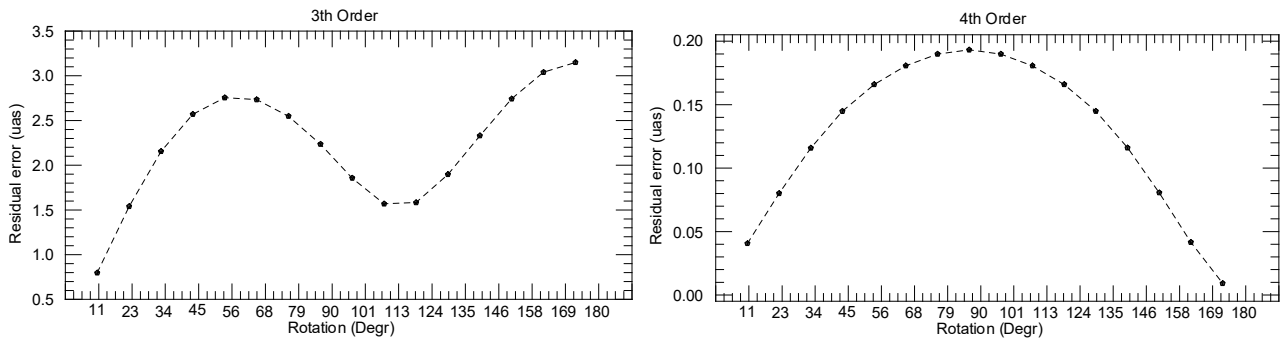


Figure 3: Astrometric residual errors for a range of field rotations (inter-epoch observations) in the circle containing the MICADO FoV. The error is the standard deviation computed as the quadratic sum of the X and Y error. Left: Residuals of a 3rd order polynomial fit. Right: Residuals of a 4th order polynomial fit.

This is the astrometric residual error showed in Figure 3 for a range of field rotation angles representative of inter-epoch observations. A 3th order polynomial is enough to model distortions considering the nominal MAORY design.

During intra-epoch observations, the optical distortions shall not smear the PSF due to field rotation and counter-rotation. Geometric distortions from the Main Path Optics are asymmetric. As the imaged sky rotates with respect to the optics during an exposure, the PSF of a point-like source on the exit focal plane follows an imperfect trajectory, which may be described as an arc of a circle, with small perturbations due to the geometric distortions from the optics. Field de-rotation only compensates for the circular part of the trajectory.

The distortion analysis considers the maximum integration time for narrow band astrometric observations at 80° of telescope elevation, i.e. 10° from zenith.

The requirement is described in the following:

- $T \approx 120$ sec. It is the maximum integration time for narrow band astrometric observations;
- $A \approx 13.7 \times (1/\cos(80^\circ)) \approx 79$ arcsec/s. It is the maximum de-rotator angular velocity;
- $T \times A \approx 2.6^\circ$. It is the maximum field rotation within a single exposure image.

During this rotation, the FWHM of the long-exposure PSF due to the MAORY optics should not increase by more than 1/10 of its nominal value.

For wavelength $\lambda = 1\mu\text{m}$, the amount of distortion shall be < 2.4 mas at the MAORY exit focal plane on the MICADO FoV (F/17.74 focal ratio).

The positions of a set of N test stars placed over a regular grid has been used to evaluate the geometric distortion. Let us define X_1, Y_1 the initial coordinates of star centroids. X_2, Y_2 the coordinates of the star centroids after the maximum astrometric exposure time (i.e. 2.6° FoV rotation and counter-rotation angle). The PSF centroids move, because of geometric distortions, by $\Delta X = (X_2 - X_1)$ and $\Delta Y = (Y_2 - Y_1)$. The vector sum of ΔX and ΔY is the geometric distortion shown in the present document.

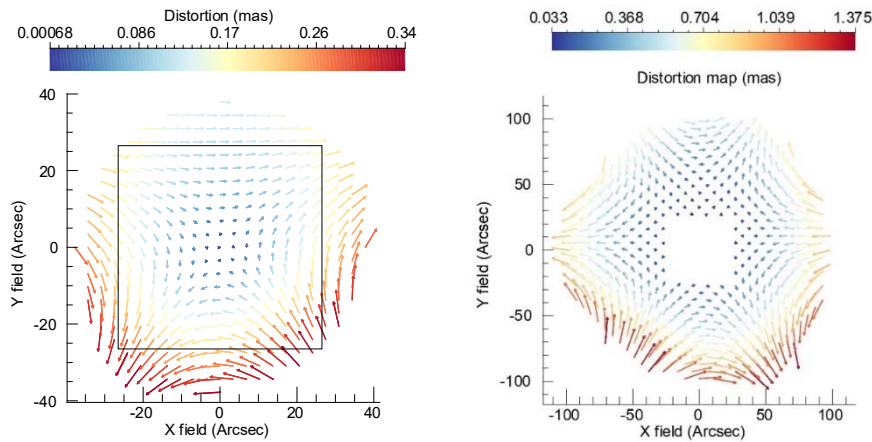


Figure 4. Distortion map at the exit port within the maximum integration time for narrow band astrometric observations (without degradation from manufacturing and alignment errors; nominal telescope design included). Left: Distortion map in the circle containing the MICADO FoV (black square). Right: Distortion map in the NGS patrol FoV

In MCAO, the position of NGSs on the NGS WFS focal plane fixes the plate scale. If the FoV is affected by optical distortion, it will introduce a differential Tip-Tilt (shift) of the NGS constellation respect to the nominal on-sky position. This translates into local plate scale distortions that will affect and potentially destroy the astrometry [6]. If the NGS WFS probes are positioned on the respective stars at the beginning of a sequence of astrometric exposures, during the image integration the stars will drift with respect to their initial position, because of the non-rotational part of the geometric distortion itself. There are a total of three plate scale modes: plate scale stretched in X and Y, respectively, and shear. Thus, if three or more reference objects are available in the field, it is possible to use them to calibrate the plate scale error. If the NGSs are used as references, differential flexure between the probes will introduce the same kind of error as the optical distortion. These errors could be defined as positioning errors and has to be properly calibrated.

To evaluate the impact of NGSs distortions on the MICADO FoV, 3 NGSs has been considered at the vertices of the equilateral triangle inscribed in the 200 arcsec FoV with different angular orientations (i.e. field rotation).

Let (X_1, Y_1) be the initial coordinates of the stars centroids, (X_2, Y_2) the coordinates of the stars due to geometric distortion after the field rotation and counter-rotation within the single astrometric image. The errors have been modelled as follows:

$$X_2 = A_x + B_x X_1 \quad (3)$$

$$Y_2 = A_y + B_y Y_1 \quad (4)$$

The coefficients (A_x, A_y) are the Tip-Tilt components of the geometric distortion, while (B_x, B_y) are the 1st order errors due to differential Tip-Tilt between the probes (plate scale). An example of induced distortions to the MICADO FoV (75 arcsec diameter) because of the considered NGSs asterism is shown in Figure 5.

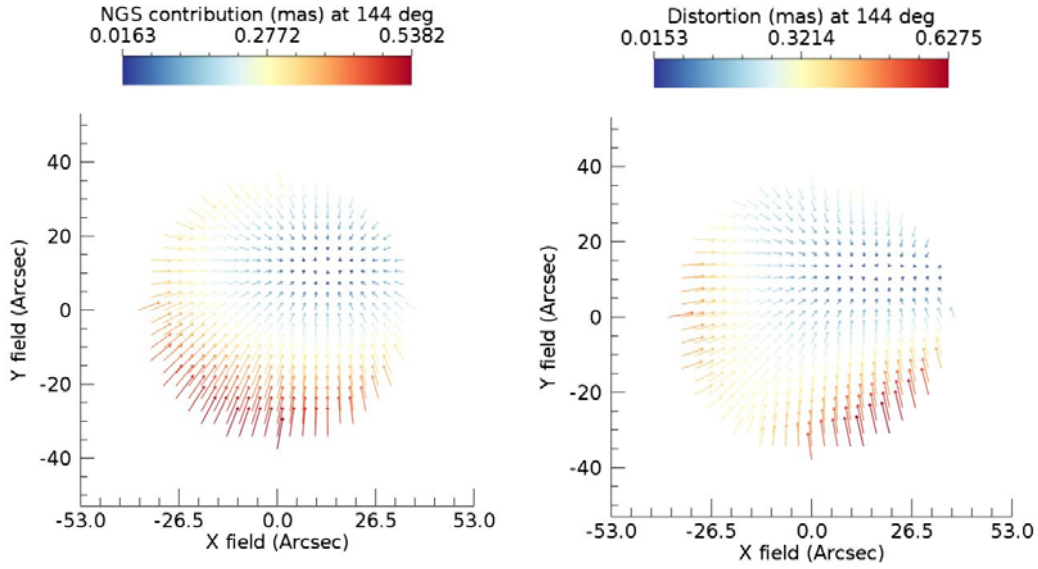


Figure 5. Left: Tip-Tilt and plate scale errors introduced to the MICADO FoV (75 arcsec diameter) due to geometric distortion of the considered NGS asterism (equilateral triangle asterism with vertices at the edge of 200 arcsec FoV diameter and rotated by 144°). Right: Distortion map for the longest single astrometric image in the MICADO FoV after adding the contribution of the NGS asterism (i.e. algebraic sum of NGS induced distortions and MICADO FoV geometric distortions)

2.4 LGS Objective wavefront error

The RMS WFE at the exit focal plane of the LGS Objective is shown in Figure 6. The maps consider all the possible range of LGS constellation angular diameter, for three different cases of Zenith angle. Fixing the LGS constellation at 45 arcsec angular diameter, Figure 7 shows the WFE vs. Zenith angle (after removal of tip-tilt and focus). In MCAO, the variation of wavefront with Zenith angle could be an issue and it has to be calibrated. The calibration procedure to remove these quasi-static aberrations from the LGS measurements might be based on temporal filtering of the LGS WFS measurements. Figure 8 shows the variation of residual RMS WFE (after removal of tip-tilt and focus) vs. Zenith angle. This variation has been considered on a timescale of 4 minutes equivalent to one degree of Zenith angle. The RMS WFE computed over the last 4 minutes in time is subtracted from the RMS WFE at each Zenith angle. The variation of WFE is indeed very small, less than 10 nm for all possible Zenith angles.

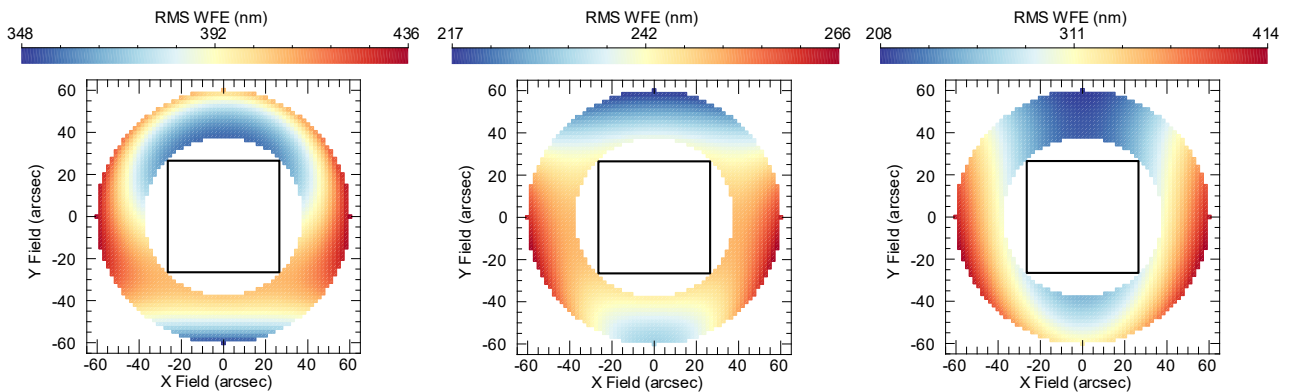


Figure 6. WFE maps at three different distances of the LGS from the telescope. From left to right: 80km – 140km – 240km. The WFE map is enclosed in a ring of inner diameter of 75 arcsec and outer diameter of 120 arcsec: this is the range within which the LGS asterism will be generated. RMS WFE without degradation from manufacturing and alignment errors; nominal telescope design included.

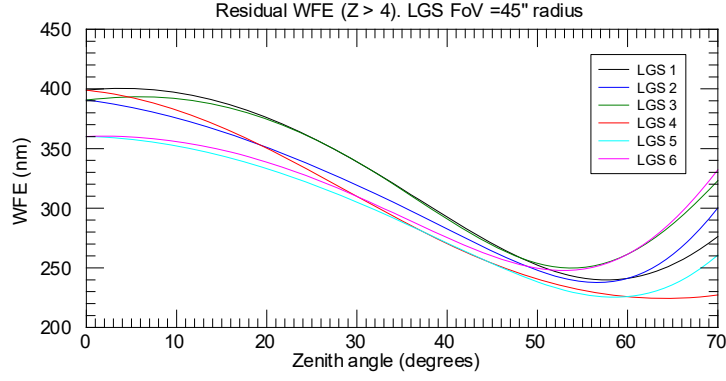


Figure 7. Residual WFE at the LGS Objective image plane (after removal of tip-tilt and focus) as a function of Zenith angle. The 6 curves correspond to an equal number of LGS, symmetrically arranged over a 45 arcsec radius FoV.

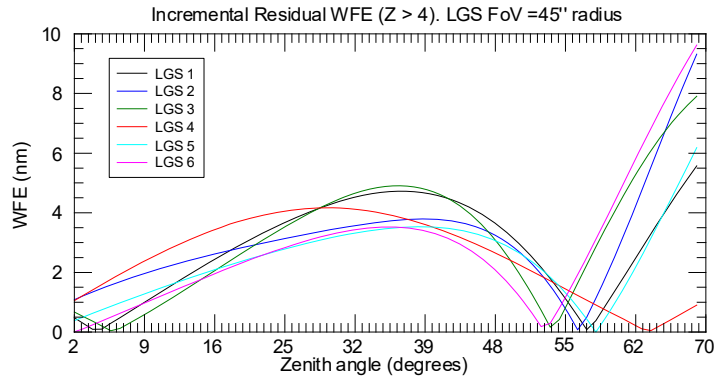


Figure 8. Variation of the residual WFE at the LGS Objective image plane (after removal of tip-tilt and focus) as a function of Zenith angle. The temporal average of the last 4 minutes is removed from the wavefront at each Zenith angle. The telescope tracks one degree every 4 minutes. The 6 curves correspond to an equal number of LGS, symmetrically arranged over a 45 arcsec radius FoV.

3. TOLERANCE ANALYSIS

3.1 Sensitivity analysis

Once defined a merit function of system performances, the sensitivity analysis considers each tolerance individually and evaluates its effect on the merit function. The introduced errors by each tolerance are combined by RSS to find the net effect of all the tolerances on the system. In terms of WFE, the sensitivity is basically the partial derivatives of the aberrations with respect to the tolerances (curvature, asphericity, thickness, decenter, etc.) multiplied by the individual tolerances.

In general, the estimated error by RSS is:

$$E = \sqrt{E_o^2 + \sum_i \left(\frac{\partial E_i}{\partial x_i} \Delta x_i \right)^2} \quad (5)$$

Where E_o is the nominal error and the sum is taken over the sensitivity of a single parameter $\partial E_i / \partial x_i$ due to its tolerance Δx_i . This method assumes that errors introduced by each individual tolerance are statistically uncorrelated. Additionally, it does not assist in defining what the tolerance values should be. Instead, it provides a translation between error limits and performance degradation.

The analysis allows to identify parameters which are highly sensitive to certain errors, such as surface curvature radii or decentres and it is also valuable to find the optimum number of compensators for required adjustments. The sensitivities

related only to available degrees of freedom (DOF) can be also used during the alignment phase of the instrument. In fact, the system requires an accurate inspection to the type of aberrations that are introduced by each DOF in order to choose the most effective compensators during the alignment.

As criterion for tolerancing, the defined merit function considers the RMS WFE referred to star centroid and adds boundary constraints on the compensators and geometric distortion in MICADO FoV as described in Section 2.

3.2 Tolerance breakdown

The tolerance analysis has been divided into 2 blocks that consider different error sources of the optical elements:

Block 1: Manufacturing errors (curvature radii and, in general, RMS surface irregularities)

Block 2: Alignment errors

The first block listed above, considers two kinds of manufacturing errors which have been categorized as:

Low order (LO) errors: these are LO deviations from the nominal optical surface and they are supposed to be partly compensated by a design re-optimization after manufacturing.

High order (HO) errors: these are HO deviations from the nominal optical surface and they are the worst offender for astrometric requirements as discussed later.

Surface irregularities are modelled by means of standard Zernike coefficients [7] whose max tolerance value is the exact RMS error of the surface. Tolerance on Zernike coefficient 11 (Z11, the "spherical" term) is equivalent to a variation on the surface conic constant. Tolerance on Zernike coefficient 4 (Z4, the "defocus" term) is equivalent to a variation on the surface curvature radii. This is true for on-axis surfaces while the combination of LO deviations from the nominal optical surface ($4 \leq \text{Zernike coefficients} \leq 45$) is equivalent to tolerances on conic constant and aspheric terms for off-axis surfaces. Tip and Tilt terms (Z2 - Z3) are not considered because they are part of tolerance Block 2. Tolerances on scratch-dig, lens bubbles and surface roughness are not considered for the scope of this paper because they mainly introduce aesthetic effects and scattered light.

Block 2 is strictly related to mechanical accuracy and precision of optical mounts and considers two kinds of tolerances:

Tolerances of assembly: these are pre-alignment tolerances related to the positioning of optical components with a laser tracker. During the alignment, some DOF are used as compensators of these tolerances to reach the required performances.

Tolerances of stability: these define the range within which each DOF is allowed to move when the system is in operation. These tolerances also refer to the minimum accuracy of compensators during the instrument alignment.

To evaluate the impact of tolerances on astrometry, a Monte Carlo simulation is mandatory. This simulation generates a series of random systems which meets the specified tolerances with a normal distribution. It is a realistic simulation of expected performance since all applicable tolerances are simultaneously and exactly considered.

For each block, a Monte Carlo simulation of 100 realization was run to investigate the system performance degradations or variations. In the case of tolerances of stability, a parabolic distribution has been used.

This tolerance analysis approach has been applied to the Main Path Optics as well as to the LGS Objective. The latter has no requirements on optical distortions and only the evaluation on RMS WFE degradation has been considered. The goal was to maintain a maximum difference respect to the nominal design below 30%. The allowed change is a 'rule of thumbs' for the adaptive optics systems tolerance analysis.

The pupil quality after the MAORY exit port, the focal aperture and the exit pupil distance variations have also been calculated. Their changes, for each tolerance block, are compliant with the requirement.

3.3 Main Path Optics manufacturing errors

Manufacturing tolerances are summarized in Table 1. A partial compensation of these tolerances can be done re-optimizing the optical design once the real values are measured after the manufacturing. This is true for irregularities modelled by Zernike coefficients in the range of $4 \leq Z \leq 11$.

For flat surfaces (dichroic and M11), the tolerance on curvature is expressed in terms of distance on the normal from the surface to the center of the curvature ("Sagitta").

Surface irregularities can be described as waviness with a given period and amplitude. In general, the period upper limit is given by the surface diameter when half cycle of waviness is over the whole surface. The period lower limit is given by the beam footprint diameter when more than one cycle of waviness is over the beam footprint and instead of additional WFE, surface irregularities causes scattered light. This is related to the surface roughness which is not considered in the analysis.

The effect on astrometry has been evaluated considering different field points. The beams footprints overlap differently on each MAORY mirror surface. As the field rotates during the observations, the beams footprints cross the static errors on each mirrors surface. The lower is the overlap of different footprints, the bigger is the difference in terms of irregularities introduced in each optical trail relative to a given field point. This error is largest for the surfaces with the largest conjugate ranges.

As the optical footprint on a surface is the smaller, the farther the surface is from the pupil plane. For MAORY, this means that it is largest for the flat folding mirror (M11) followed by the first mirror after the entrance focal plane (M6). The surface waviness period and amplitude which mostly effect the astrometric accuracy is modelled by Zernike coefficients greater than 28 (Table 1) as they introduce high order residuals on the polynomial fit.

Given the values listed in Table 1, about 12% of the residuals are due to the Zernike coefficients in the range $29 \leq Z \leq 45$, 33% of the residuals are due to $46 \leq Z \leq 120$, the rest is due to $121 \leq Z \leq 230$.

However, the sensitivity of surface irregularities on the RMS WFE is overall greater than on optical distortion, establishing the wavefront degradation as the leading parameter on tolerance analysis of surface irregularities.

Figure 9 shows the residual errors of the polynomial fit due to manufacturing tolerances. Inter-epoch observations are represented by the range of field rotation angles.

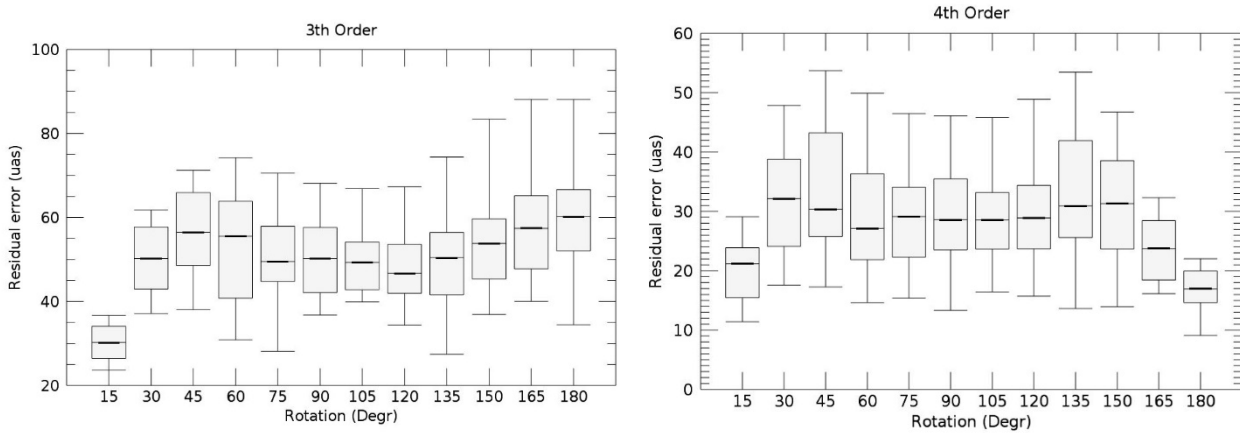


Figure 9: Astrometric residual errors for a range of field rotations in the circle containing the MICADO FoV. The error is the standard deviation computed as the quadratic sum of the X and Y error. Box plots show minimum and maximum values and quartiles of Monte Carlo trials distribution. The boxes width is related to the power spectrum of Zernike coefficients. Greater residuals are related to larger RMS irregularity in the highest Zernike coefficient range.

The effect on geometric distortion is negligible (~ 0.2 mas) regarding the PSF smear in a single exposure image within the MICADO FoV. But, since distortions are not linear with the FoV diameter, the effect of induced distortions by MCAO with NGSs could be an issue. The simplistic analysis described in Section 2.3 has been done considering the worst Monte Carlo realization. It still satisfies the geometric distortion requirement as shown in Figure 10 and no calibrations are here considered.

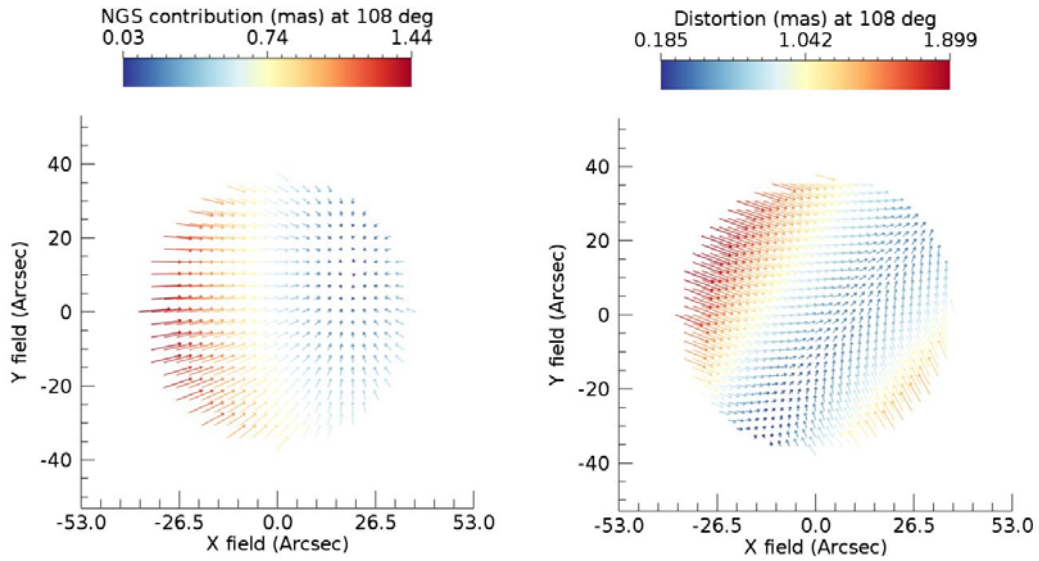


Figure 10. Same of Figure 5 but considering the manufacturing tolerances. This is the worst Monte Carlo realization for geometric distortion.

Table 1: Main Path Optics manufacturing tolerances. Spherical aberration for flat surfaces is included in the budget of irregularities.

Manufacturing tolerances					
Curvature radius			± 0.1 %		
Sag of flat surfaces (residual curvature)			± 316 nm		
<i>Spherical aberration (RMS error)</i>					
All mirrors with optical power			5 nm		
<i>Surface irregularity (RMS error)</i>					
Mirror #	Astigmatism + Coma + Trefoil	Zernike range Z ₁₂ to Z ₂₈	Zernike range Z ₂₉ to Z ₄₅	Zernike range Z ₄₆ to Z ₁₂₀	Zernike range Z ₁₂₁ to Z ₂₃₀
M6	24 nm	5 nm	5 nm	4 nm	4 nm
M7	18 nm		3 nm		
M8	15 nm		5 nm		
M9	14 nm		3 nm		
M10	20 nm		3 nm		
M11	23 nm		5 nm		
Dichroic	11 nm		5 nm		

The effect of these tolerance on the RMS WFE is about 10 nm. It is the difference between the mean RMS WFE of nominal design over the 200 arcsec FoV diameter and the mean RMS WFE of the Monte Carlo trials considering the same FoV.

3.4 Main Path Optics alignment errors

Alignment tolerances are summarized in Table 2. The DOF, used as compensators of misalignments, are rigid body motions of each optical surface that can be controlled by active components (i.e. hexapod or similar device) when needed. These are:

- Tip-Tilt about x and y axes
- Decenter in x and y axes
- Axial position

where x and y are two axes orthogonal to the optical element axis.

The compensators shall work in combination with a metrology system or other measurement method which provides the necessary information to change the optical path according to estimated misalignments.

The rigid body motions are respect to the local coordinate system of each optical component. The axial position (Z) has to be intended as the relative distance between pairs of subsequent optical elements (e.g. M6-M7; M7-M8 and so on).

During the instrument alignment, the compensators have to be repeatable within the range defined for stability. Compensation motions used during the alignment are listed in Table 3. The analysis of performances degradation has been done using a parabolic distribution for Monte Carlo simulation since it yields selected values that are more likely to be at the extreme ends of the tolerance range.

Table 2: Tolerances of Main Path Optics degrees of freedom. Required accuracy during system mechanical assembly and required stability after system alignment achieved with compensators (listed in Table 3).

Tolerances of stability	
X-Y Tilts (M7 – M9 – M10 – Dichroic)	$\pm 30 \mu\text{rad}$
X-Y Tilts (M6)	$\pm 87.5 \mu\text{rad}$
X-Y Tilts (M8 – M11)	$\pm 17.5 \mu\text{rad}$
Z Tilt (All optics rotation around optical axis)	$\pm 30 \mu\text{rad}$
Axial position (M8 repeatability)	$\pm 0.1 \text{ mm}$
Axial position (All optics repeatability except M8)	$\pm 0.2 \text{ mm}$
Axial position (compensated by re-focus)	$\pm 1 \text{ mm}$
X-Y Decenters (All optics)	$\pm 0.1 \text{ mm}$
Tolerances of assembly	
X-Y Tilts	$\pm 0.96 \text{ mrad}$
Axial position	$\pm 1 \text{ mm}$
X-Y Decenters	$\pm 0.25 \text{ mm}$
Z Tilt (rotation around optical axis)	$\pm 0.96 \text{ mrad}$

As the manufacturing tolerances, the effect of these tolerance on the RMS WFE is about 10 nm. It is the difference between the mean RMS WFE of nominal design over the 200 arcsec FoV diameter and the mean RMS WFE of the Monte Carlo trials considering the same FoV. This degradation is only related to tolerances of stability since after the assembly, the alignment residual, reached with compensators, is less than 2 nm in terms of mean RMS WFE.

Considering the optical distortion, the effect of these tolerances is negligible. The mis-alignments, introduced during a single exposure image, shift the optical axis in a way that it is no more aligned with the field de-rotator mechanical axis. The mismatch generates star trails but can be compensated by the MCAO which sees a global Tip-Tilt on NGSs.

Table 3: List of compensators and required motion range for Main Path Optics alignment.

Compensators: M6 – M7 – M8 – M9	Motion range
X-Y Tilts	± 5 mrad
Axial position (M8)	± 1 mm

3.5 LGS Objective manufacturing errors

In the tolerance analysis, the main differences between the LGS Objective and the Main Path Optics are:

1. The LGS Objective contains lenses in the optical path;
2. The RMS WFE of the LGS Objective shall exclude the Tip-Tilt and defocus terms;
3. Geometric distortion is not an issue for the LGS Objective;
4. LGSs are not focused at infinity but in a range of finite altitudes.

Manufacturing tolerances are summarized in Table 4. The effect of these tolerance on the RMS WFE has been evaluated on 6 LGSs at 45 arcsec field radius. The Monte Carlo results, in terms of residual RMS WFE, are shown in Figure 11.

Table 4: LGS Objective. Lenses manufacturing tolerances

Manufacturing tolerances		
Curvature radius		± 0.1 %
Sag of flat surfaces (residual curvature)		± 316 nm
Wedge		± 87.5 μ rad
Lens front-back surface centring		± 0.05 mm
Glass thickness		± 0.1 mm
Spherical aberration (RMS error)		10 nm
Surface irregularity (RMS error)	Astigmatism + Coma + Trefoil	25 nm
	Secondary astigmatism + Higher orders	5 nm
Glass refractive index		$\pm 10^{-3}$
Glass Abbe number		± 1 %

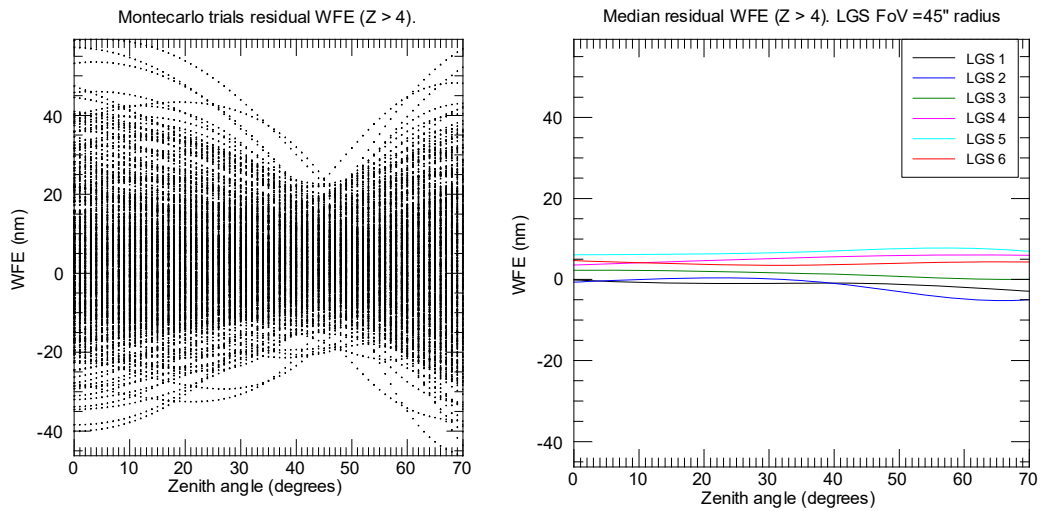


Figure 11. Monte Carlo trials for manufacturing errors of the LGS Objective optics. Left: variation of WFE at the LGS Objective image plane with respect to the nominal value as a function of Zenith angle. Right: mean values of the left plot, different colours correspond to different positions around the 45 arcsec circle FoV of the LGSs.

3.6 LGS Objective alignment errors

Alignment tolerances are summarized in Table 1. The alignment of the LGS Object is foreseen by using only the DOF of Lens 5. In this case, after the assembly, the alignment residual, reached with compensators, is less than 20 nm in terms of mean RMS WFE. The Monte Carlo results, in terms of residual RMS WFE due to tolerances of stability, are shown in Figure 12.

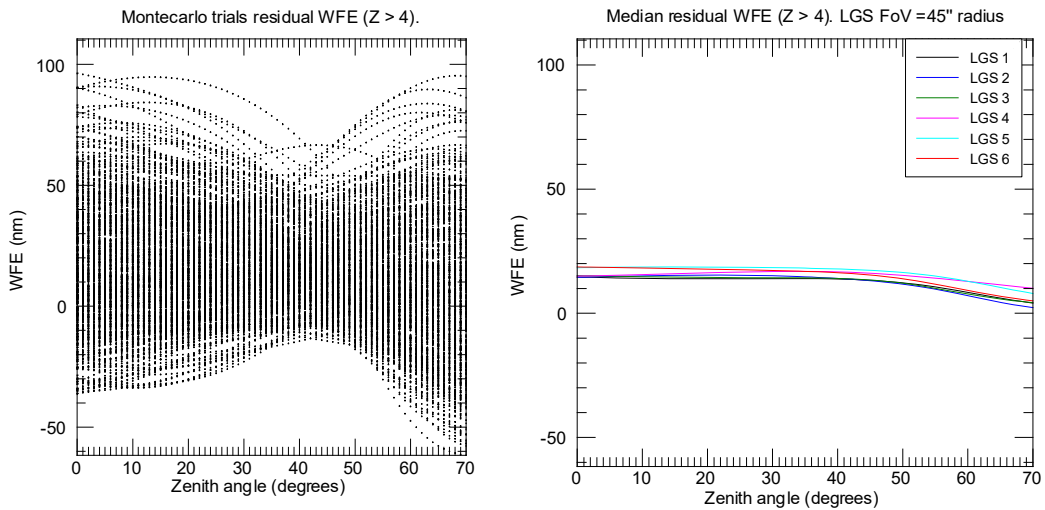


Figure 12. Same of Figure 11 but considering the tolerances of stability.

Table 5: Tolerances of LGS Objective degrees of freedom. Required accuracy during system mechanical assembly and required stability after system alignment achieved with compensators (listed in Table 6).

Tolerances of stability	
Axial position	$\pm 50 \mu\text{m}$
X-Y Decenters	$\pm 50 \mu\text{m}$
X-Y Tilts	$\pm 87.5 \mu\text{rad}$
Z Tilt	$\pm 0.17 \text{ mrad}$
Tolerances of assembly	
X-Y Decenters (All Lenses)	$\pm 0.1 \text{ mm}$
X-Y Tilts (Lenses 1 – 2 and folding mirror)	$\pm 0.17 \text{ mrad}$
X-Y Tilts (Lenses 3 – 4)	$\pm 87.5 \mu\text{rad}$
Z Tilt (All lenses)	$\pm 0.17 \text{ mrad}$
Axial Position	$\pm 0.1 \text{ mm}$

Table 6: List of compensators and required motion range for LGS Objective.

Compensator: Lens 5	Motion range
Axial position	$\pm 5 \text{ mm}$
X-Y Decenters	$\pm 0.5 \text{ mm}$
X-Y Tilts	$\pm 5 \text{ mrad}$

4. CONCLUSIONS

The presented MAORY optical performances through tolerance analysis has been essential to define the opto-mechanical requirements to be used in the procurement process. A summary in terms of expected performances degradation is listed in Table 7.

The analysis results will be refined during the MAORY project phase C (e.g. relaxing some tolerances) considering also the preliminary cost breakdown provided by external companies.

The main path optics is expected to undergo very minor changes (e.g. FoV and thus, mirror diameters) in the final design phase while a major change could interest the LGS Objective. Its baseline design has been developed with a tight requirement on the residual quasi-static WFE. The main aspect to be considered, from the technical point of view, is the level of residual WFE and the effectiveness of the calibration procedures to remove it from the LGS measurements. If larger WFE is confirmed to be acceptable, the design could be simplified, allowing significant cost reduction and possible easier AIV procedures.

Table 7: Expected wavefront degradation due tolerances.

Main Path Optics		Mean RMS WFE degradation	Notes
Manufacturing	LO irregularities	8 nm	$4 \leq \text{Zernike modes} \leq 11$ partly compensated by design re-optimization
	HO irregularities	7 nm	Worst offender for astrometry $29 \leq \text{Zernike modes} \leq 230$
Alignment	Assembly	2 nm	Compensation applied during alignment by M6 – M7 – M8 – M9
	Stability	10 nm	Required during instrument operation
LGS Objective			
Manufacturing	LO+HO irregularities	10 nm	$4 \leq \text{Zernike modes} \leq 11$ partly compensated by design re-optimization
Alignment	Assembly	20 nm	Compensation applied during alignment by Lens 5
	Stability	30 nm	Required during instrument operation

5. RIFERENCES

- [1] E. Diolaiti e others, «MAORY: a multi-conjugate adaptive optics relay for the E-ELT,» *The Messenger*, vol. 140, pp. 28-29, 2010.
- [2] R. Gilmozzi e J. Spyromilio, «The 42m european elt: status,» in *SPIE Astronomical Telescopes+Instrumentation*, 2008.
- [3] R. Davies e M. I. C. A. D. O. Team, «MICADO: the E-ELT adaptive optics imaging camera,» *arXiv preprint arXiv:1005.5009*, 2010.
- [4] M. Lombini, M. Patti, P. Ciliegi, F. Cortecchia, E. Diolaiti, P. Feautrier e others, «Optical design of the post focal relay of MAORY,» in *SPIE Optical Design and Engineering VII*, 2018.
- [5] M. Lombini, «Laser Guide Star Objective of MAORY,» in *Proceedings of the Adaptive Optics for Extremely Large Telescopes 5*, 2017.
- [6] B. Neichel, F. Rigaut, A. Serio, G. Arriagada, M. Boccas, C. d'Órgeville, V. Fesquet, C. Trujillo, W. N. Rambold, R. L. Galvez e others, «Science readiness of the Gemini MCAO system: GeMS,» in *SPIE Astronomical Telescopes+ Instrumentation*, 2012.
- [7] R. J. Noll, «Zernike polynomials and atmospheric turbulence,» *JOSA*, vol. 66, pp. 207-211, 1976.